Supporting Information

Isostatic Pressure Assisted Nanocasting Preparation of Zeolite Templated Carbon for High-Performance and Ultrahigh Rate Capability Supercapacitors

Chunlin Teng,[a] Yi Han,[a] Guangying Fu,[a] Jibo Hu,[a] Haibing Zheng,[a] Xihong Lu,[a,b] and Jiuxing Jiang*[a]*

1. Characterization

The microstructures of ZTCs were observed by scanning electron microscope (SEM SU8010) and transmission electron microscope (JEM-2010HR) at an acceleration voltage of 300 kV. The ordered structure of the ZTCs was analyzed with a powder X-ray diffractometer (SmartLab) using Cu-Kα radiation generated at 40 kV and 30 mA. Nitrogen isotherms of the samples were measured at 77 K on a volumetric sorption analyzer (micromeritics ASAP 2020 PLUS HD88). The specific surface areas (SSA) were calculated using the Brunauer–Emmett–Teller (BET) method using the data in the relative pressure range of 0.05~0.15. The total pore volumes (V_{total}) were calculated from the N_2 adsorption amount at P/P_0 = 0.995. Micropore volume (V_{micro}) was calculated by t-plot method. Mesopore volume (V_{meso}) was determined by subtracting the micropore volume from the total pore volume. Pore size distributions (PSDs) were obtained from the adsorption isotherms using the nonlocal density functional theory (NLDFT) model, assuming a slit pore shape. Raman spectra were recorded on a Laser Micro-Raman Spectrometer (Renishaw in Via) with a laser excitation wavelength of 633 nm. The composition and functional group distribution of the samples were determined by X-ray photoelectron spectroscopy (XPS, ESCALab250, USA) and elemental analysis (EA, Vario EL).

In three-electrode tests cyclic voltammetry (CV) and chronopotentiometry (CP) were conducted in a standard electrolytic cell with a conventional three-electrode configuration using CHI 660D electrochemical workstation (CH Instruments Inc.) and 6 M KOH aqueous solution as electrolyte. ZTCs on nickel foam were used as working electrode. Graphite rod (~5 mm diameter) and Hg/HgO electrode were used as counter electrode and reference electrode, respectively. Electrochemical impedance spectroscopy (EIS) was conducted in a range of 0.1 Hz to 100 kHz at open circuit potential with an amplitude voltage of 5 mV.

The EASA for each system was estimated from the electrochemical double-layer capacitance of the electrode surface by CV method. The CV test at different scan rate in a potential range of 0.1 V where no apparent faradaic processes occur.

2. Calculation

2.1 Single Electrode Capacitance calculated based on chronopotentiometry (CP)

Capacitance of a single electrode from CP test is calculated from equation S1:

$$C_s = I \triangle t / \triangle V \qquad \text{(Equation S1)}$$

Here C_s is the specific capacitance (F g^{-1}), I is the discharge current density (A g^{-1}), $\triangle t$ is the discharge time (s) and $\triangle V$ is the potential window (V).

2.2 capacitive current and diffusion-controlled current

The total capacitance of CV curve includes the capacitive (k_1) and diffusion (k_2) controlled contributions which can be separated using the equation S2:[1]

$$i(\mathrm{V}) = k_1 + k_2\, v^{1/2} \qquad \text{(Equation S2)}$$

Where i (V) is current, v is the scan rate, k_1v is the surface capacitive current and $k_2v^{1/2}$ is the diffusion-controlled current. Through fitting the equation carefully **(Fig. S3)**, the contribution of the capacitive and diffusion current can be obtained.

2.3 Electrochemically Active Surface Area (EASA)

The double-layer charging current i_c is equal to the product of the scan rate, v, and the electrochemical double-layer capacitance, C_{dl}, as given by equation S3:[2]

$$i_c = v\, C_{dl} \qquad \text{(Equation S3)}$$

Fig. 4f displays anodic charging current (i) measured at -0.85 V in CV curves as a function of the scan rate (v) for all electrodes. The slope of anodic charging current densities-scan rate curve is in direct equal to C_{dl}, which proportion to EASA.[3]

$$\text{EASA} = \frac{C_{dl}}{C_s} \qquad \text{(Equation S4)}$$

where C*s* is the specific capacitance measured for the sample with an atomically smooth planar surface, approximately 60 μ F cm^{-2}.[2]

2.4 C' and C'' capacitance

C' the real part of the capacitance and C" the imaginary part of the capacitance were calculated by using the following equation (S5) and (S6).[4]

$$C' = \frac{-Z''(\omega)}{\omega\,|Z(\omega)|^2} \qquad \text{(Equation S5)}$$

$$C'' = \frac{Z'(\omega)}{\omega\,|Z(\omega)|^2} \qquad \text{(Equation S6)}$$

Where ω is pulsation frequency, $Z'(\omega)$ and $Z''(\omega)$ are the real part and the imaginary part of the impedance, respectively. $Z(\omega) = Z'(\omega) + jZ''(\omega)$, defined as: $Z'^2 + Z''^2 = |Z(\omega)|^2$.

2.5 ZTC-P300-SSC

The energy density (E_s) and average gravimetric power density (P_s) were calculated by using the following equation (S7) and (S8):

$$E_s = \frac{1}{2} C_s \triangle V^2 \qquad \text{(Equation S7)}$$

$$P_s = \frac{E_s}{\triangle t} \qquad \text{(Equation S8)}$$

Reference

1 Y. Wang, Y. Song and Y. Xia, *Chem. Soc. Rev.*, 2016, **45**, 5925.

2 J. D. Benck, Z. Chen, L. Y. Kuritzky, A. J. Forman and T. F. Jaramillo, *ACS Catal.*, 2012, **2**, 1916-1923.

3 C. C. McCrory, S. Jung, J. C. Peters and T. F. Jaramillo, *J. Am. Chem. Soc.*, 2013, **135**, 16977-16987.

4 P. L. Taberna, P. Simon and J. F. Fauvarque, *J. Electrochem. Soc.*, 2003, **150**, A292-A300.

3. Supplementary Table

Table S1. Carbon amounts in the carbon/zeolite composites, Elemental analysis of the ZTC carbons, specific surface areas and pore volumes of the carbon replicas.

	Carbon amount (wt.%) [a]	C (%)	N (%)	BET ($m^2 g^{-1}$)	V_{total} ($cm^3 g^{-1}$)	V_{micro} ($cm^3 g^{-1}$)	V_{meso} ($cm^3 g^{-1}$)
ZTC-P0	7	80.45	3.38	844	0.515	0.412	0.103
ZTC-P150	9.8	75.7	3.49	1130	0.702	0.585	0.117
ZTC-P300	14	80.44	6.27	2169	1.339	1.102	0.237
ZTC600-P300	10	75.47	4.04	1140	0.775	0.443	0.332
ZTC800-P300	11.05	81.81	3.5	1345	0.823	0.242	0.581

a Determined by TGA from the weight loss of the carbonaceous part of the carbon/zeolite composite by oxidation in air in the range 300–800°C. Carbon amount (%) = the loss weight / the mass of carbon/zeolite composite.

Table S2. Comparison of electrochemical performance of reported carbon-based supercapacitors.

Supercapacitor	electrolyte	Specific capacity (F g^{-1}) (single electrode)	Energy density (Wh kg^{-1})	Rate performance (%)	Ref.
ZCT-P300	6 M KOH	253 (1.25A g^{-1})	7.5 at 625 W kg^{-1}	65% (1.25 to 62.5 A g^{-1})	This work
PZCC (phosphorus-doped carbon)	6 M KOH	195 (1 A g^{-1})	4.7 at 125 W kg^{-1}	68% (1 to 10 A g^{-1})	41
cMR-rGOth (3D reduced graphene oxide)	-	210 (0.5 A g^{-1})	-	68% (1 to 10 A g^{-1})	42
CCS/CCL (chitosan/cellulose carbon cryogel)	6 M KOH	150.4 (1 A g^{-1})	-	-	43
NiOx/CNF (Nickel/carbon nanofoam composite)	1 M Na_2SO_4.	150 (1 A g^{-1})	-	54% (1 to 3 A g^{-1})	44
PCNFs	0.5 M H_2SO_4	104.5 F g^{-1} (0.2 A g^{-1})	3.22 600 W kg^{-1}	56.5% (1 to 10 A g^{-1})	45
NPCHSs	6 M KOH	232 (1 A g^{-1})	-	68% (1 to 10 A g^{-1})	46
HPAC	6 M KOH	309 (0.5 A g^{-1})	-	55% (0.5 to 16 A g^{-1})	47
NHPC	6 M KOH	234 (0.5 A g^{-1})	9.43 at 630 W Kg^{-1} .	57 % (0.5 to 10 A g^{-1})	7
IMPC	1 M H_2SO_4	258 (0.5 A g^{-1})	3.1 at 13600 W kg^{-1}	58% (0.5 to 30 A g^{-1})	34
CNS-800	6 M KOH	227 (0.5 A g^{-1})	7.8 at 0.25 kW kg^{-1})	78% (0.5 to 20 A g^{-1})	35
U-GAs	1 M H_2SO_4	181 (1 mV s^{-1})	5.9 1490 W kg^{-1}	63.5% (1 to 100 mV s^{-1})	54
Carbon-PtNs	-	-	3.3	-	55

			288 W kg^{-1}		
SAGC	-	149	4.297 173 W kg^{-1}	-	56
AC-TA-700	1M H_2SO_4	233 2 mV s^{-1}	4.2 at 1500 W kg^{-1}	80% (2 to 500 mV s^{-1})	57
MBARS-IC/rGO@CF	1 M H_2SO_4	178 (0.05 A g^{-1})	3.89 at 1250 W kg^{-1}	63.5% (0.05 to 2.5 A g^{-1})	58
rGO-CH1		-	5.2 280 W kg^{-1}		59

4. Supplementary Figures

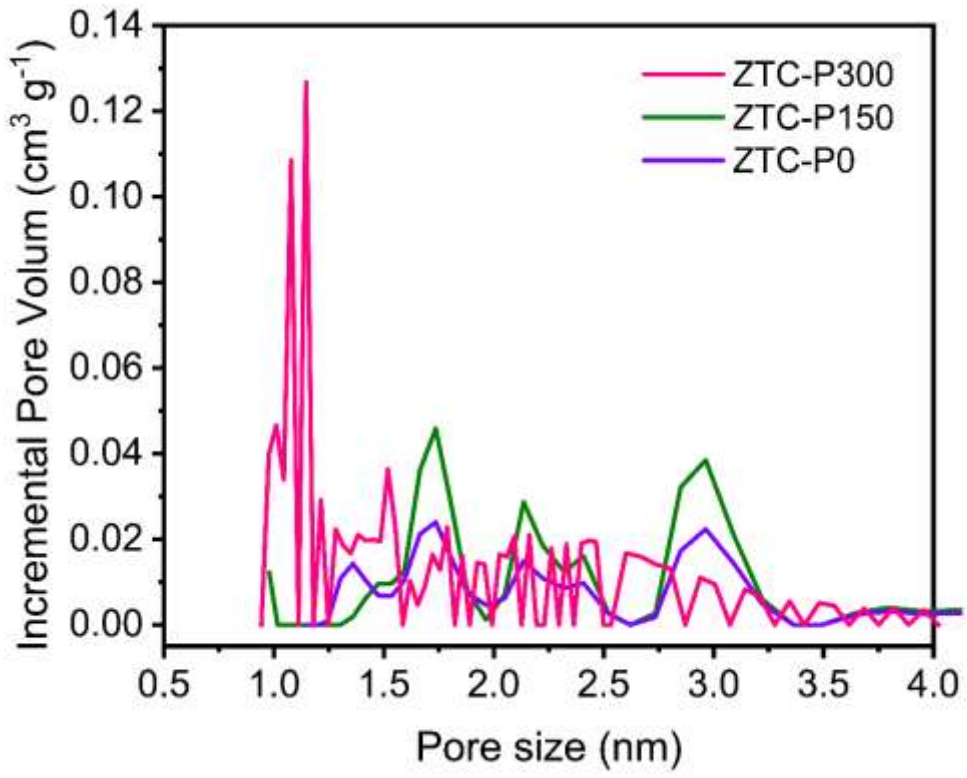

Fig.S1 Pore size distributions (PSDs) for ZTC-P300, ZTC-P150 and ZTC-P0

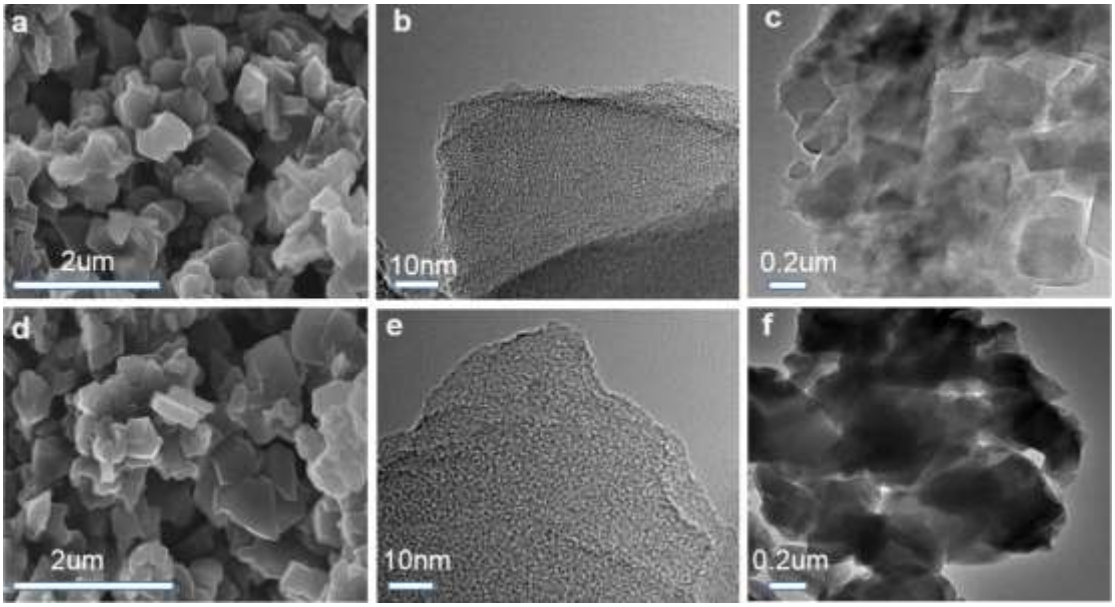

Fig. S2 (a) (d) SEM images of ZTC-P0 and ZTC-P150 respectively, (b)(c) HRTEM images of ZTC-P0, (e) (f) HRTEM images of ZTC-P150.

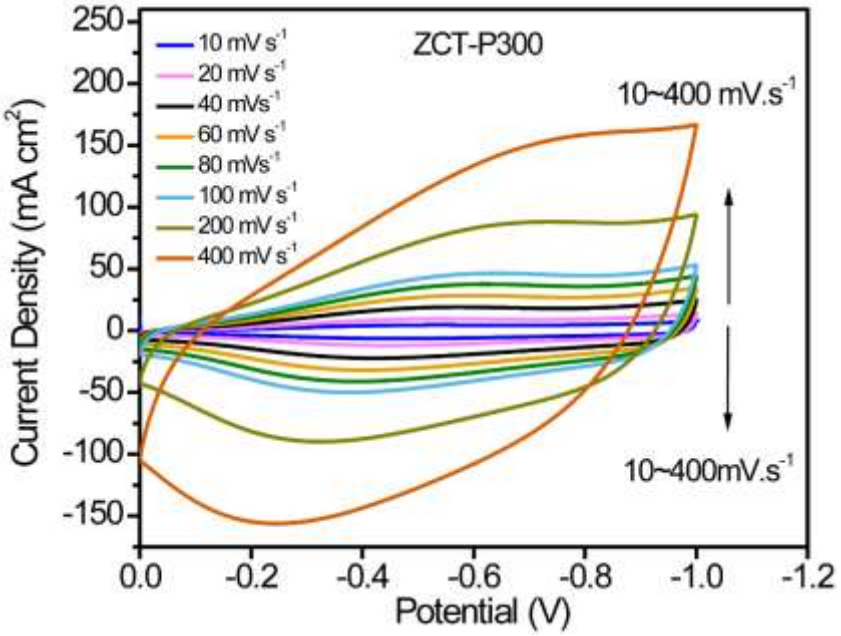

Fig. S3 CV curves of ZTC-P300 electrode at scan rates from 10 mV s^{-1} to 400 mV s^{-1} in three-electrode tests.

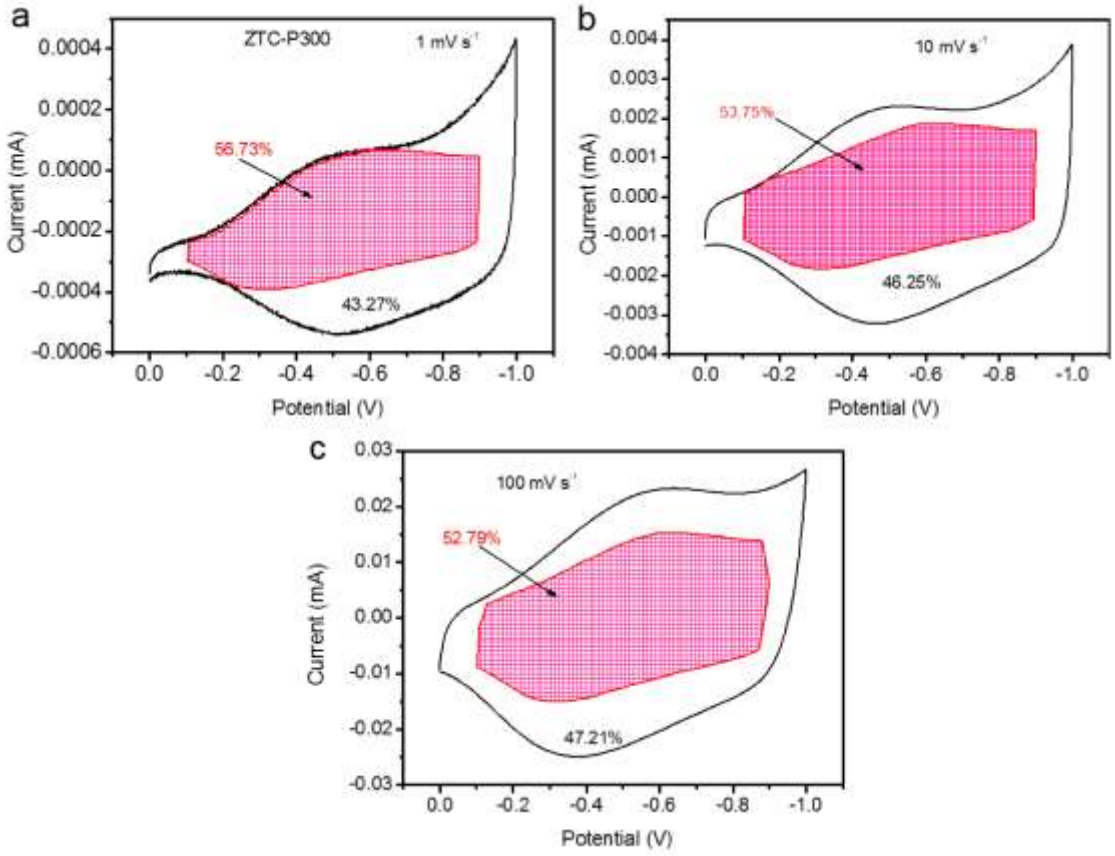

Fig. S4 The separation of capacitive and diffusion current for ZTC-P300 at a scan rate of 1 mV s^{-1}, 10 mV s^{-1} and 100 mV s^{-1}. The red part presents the capacitive contribution.

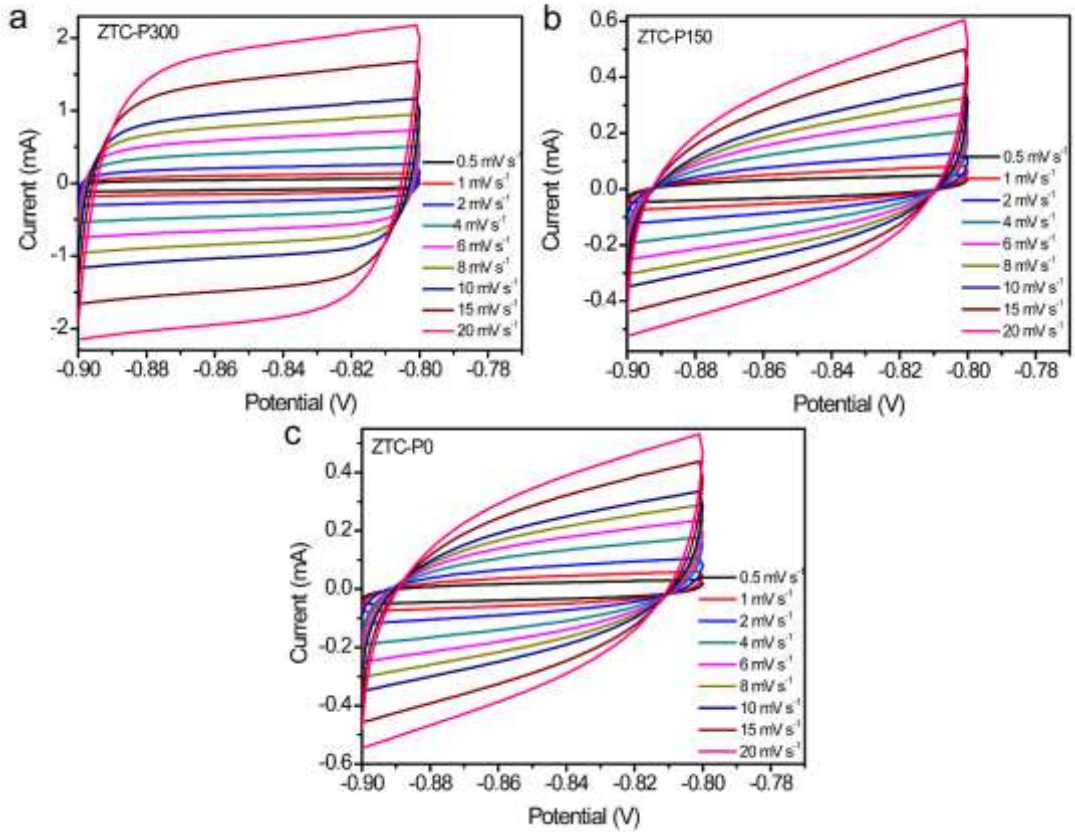

Fig. S5 Double-layer capacitance measurements for determining electrochemically active surface area for ZTCs electrodes from voltammetry in 6 M KOH. Cyclic voltammogram curves were measured in a non-faradaic region of the voltammogram at the different scan rates.

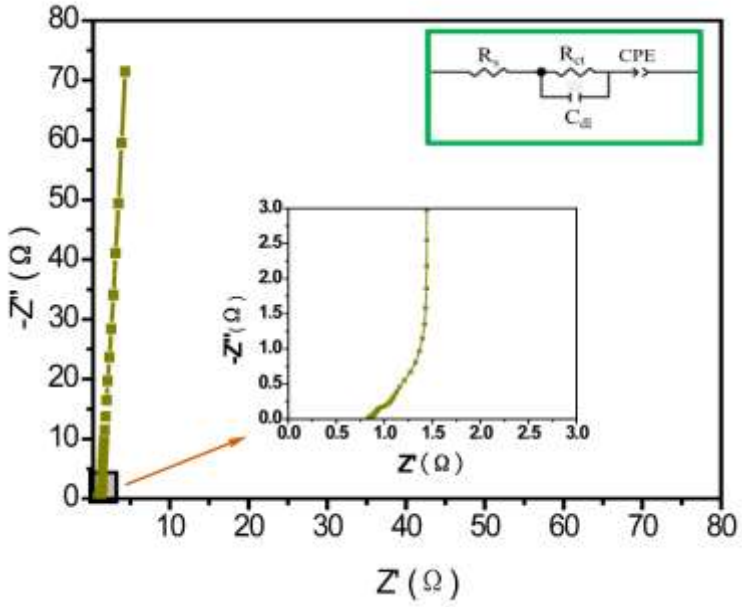

Fig. S6 Electrochemical impedance spectroscopy of Nyquist plot for ZTC-P300-SSC device together with the circuit diagram in the inset.

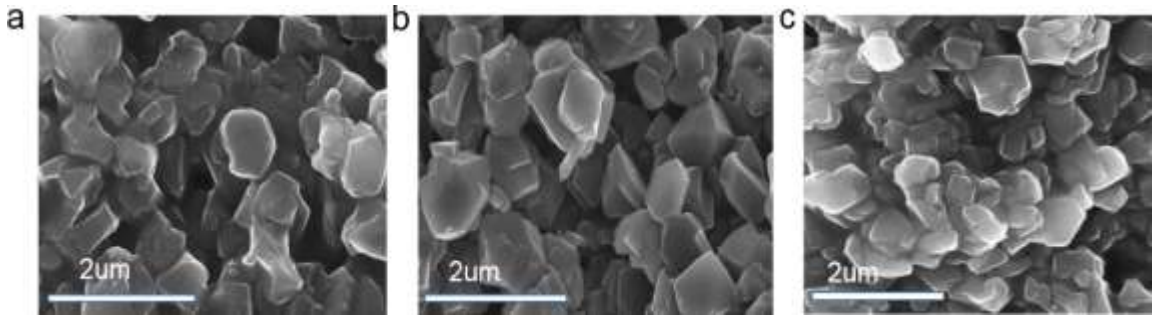

Fig. S7 (a), (b), (c) SEM images of ZTC600-P300, ZTC-P300 and ZTC800-P300, respectively.

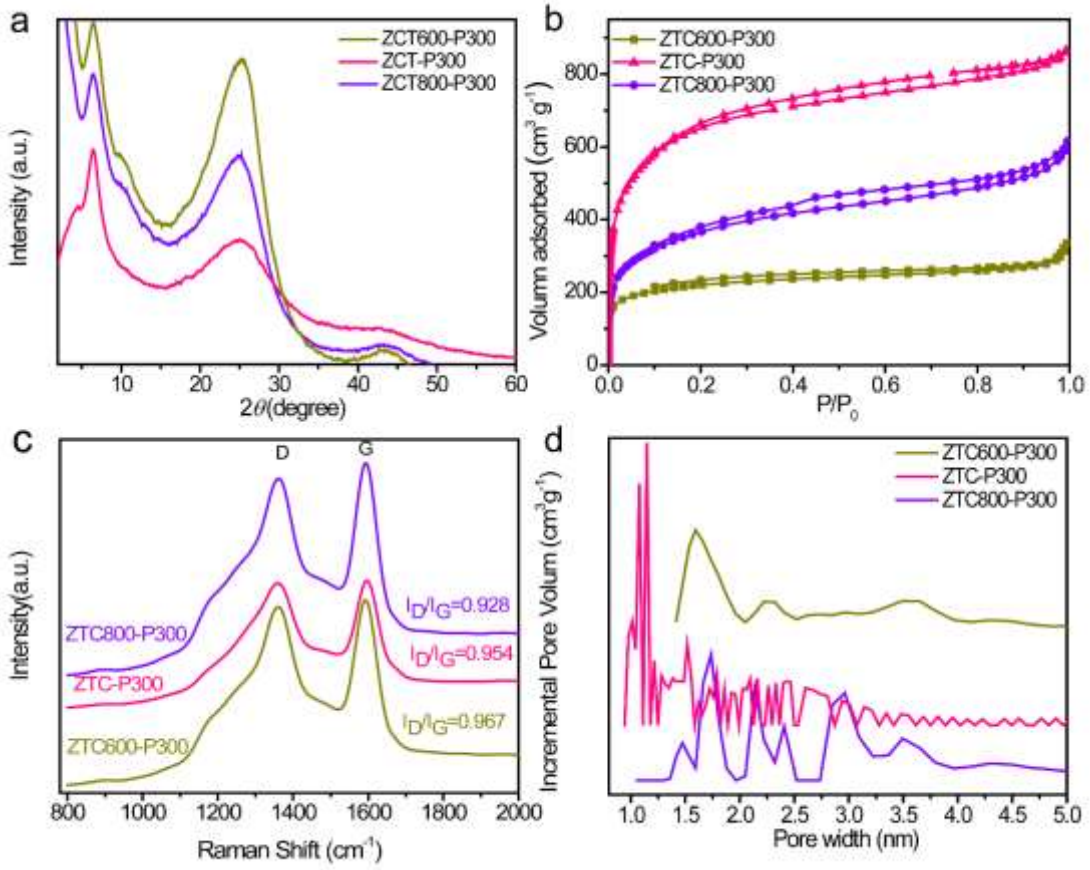

Fig. S8 (a) XRD patterns, (b) N_2 sorption isotherms, (c) Raman spectra and (d) PSDs of ZTC600-P300, ZTC-P300 and ZTC800-P300 samples.

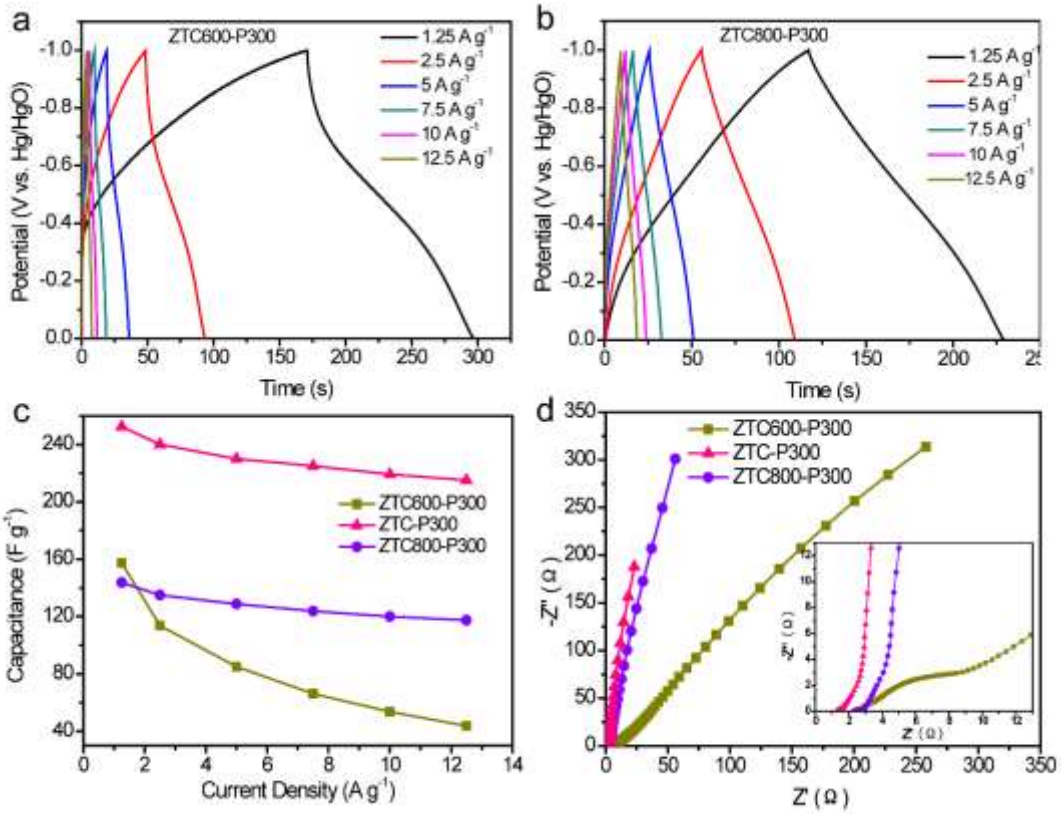

Fig. S9 Three-electrode system electrochemical test of ZTC600-P300, ZTC-P300 and ZTC800-P300 samples: (a), (b) GCD curves at different current density. (c) Specific capacitances at different current density. (d) Electrochemical impedance spectroscopy of Nyquist plots